Seizure Characterisation using Frequency Dependent Multivariate Dynamics

T. Conlon [a], H.J. Ruskin [a], M. Crane [a],
[a] *Dublin City University, Glasnevin, Dublin 9, Ireland*

Abstract

The characterisation of epileptic seizures assists in the design of targeted pharmaceutical seizure prevention techniques and pre-surgical evaluations. In this paper, we expand on recent use of multivariate techniques to study the cross-correlation dynamics between electroencephalographic (EEG) channels. The Maximum Overlap Discrete Wavelet Transform (MODWT) is applied in order to separate the EEG channels into their underlying frequencies. The dynamics of the cross-correlation matrix between channels, at each frequency, are then analysed in terms of the eigenspectrum. By examination of the eigenspectrum, we show that it is possible to identify frequency dependent changes in the correlation structure between channels which may be indicative of seizure activity.

The technique is applied to EEG epileptiform data and the results indicate that the correlation dynamics vary over time and frequency, with larger correlations between channels at high frequencies. Additionally, a *redistribution* of wavelet energy is found, with increased fractional energy demonstrating the relative importance of high frequencies during seizures. Dynamical changes also occur in both correlation and energy at lower frequencies during seizures, suggesting that monitoring frequency dependent correlation structure can characterise changes in EEG signals during these. Future work will involve the study of other large eigenvalues and inter-frequency correlations to determine additional seizure characteristics.

Key words: Cross-Correlation, Wavelet Multiscaling, EEG, Epilepsy, Eigenspectrum

1. Introduction

In recent years, the application of the equal-time correlation matrix to a variety of multivariate data sets such as financial data [1–4], electroencephalographic (EEG) recordings [5–11], magnetoencephalographic (MEG) recordings [12] and others has been studied extensively. The dynamics of such systems are characterised by a continuously varying level of synchronisation between different subsets of the system. The degree of synchronisation is dependent on the length of time-series studied, the granularity of the data and the amount of noise in the system, amongst other things.

Equal-time cross-correlation matrices have been shown to characterise dynamical changes in nonstationary multivariate time-series, [8]. It was demonstrated that, as the synchronisation of k individual time-series within an $M-$dimensional multivariate time-series increases, this causes a repulsion between eigenstates of the correlation matrix, in which k levels participate. Through the use of artificially created time-series with pre-defined correlation dynamics, it was found that there exist situations where the relative change of eigenvalues from the lower edge of the spectrum is greater than that of the large eigenvalues, implying that the information drawn from the smaller eigenvalues is more relevant as an in-

Email addresses: tconlon@computing.dcu.ie (T. Conlon), hruskin@computing.dcu.ie (H.J. Ruskin), mcrane@computing.dcu.ie (M. Crane).

dicator of event activity. An examination of shifts in the eigenspectrum of the cross-correlation matrix between epileptic seizure time-series, also revealed that information about the correlation dynamics is reflected in both the lower and upper eigenstates.

The application of the equal-time correlation matrix to EEG seizure time-series was used to study temporal dynamics for a large sample of focal onset epileptic seizures, [10]. It was shown that the zero-lag correlations between multichannel EEG signals tend to decrease during the first half of a seizure and increase gradually before the seizure ends. This work was further extended to the case of *Status Epilepticus*, where the equal-time cross-correlation matrix was used to assess neuronal synchronisation prior to seizure termination, [11].

It was demonstrated, for particular examples, that information about cross-correlations can be found in the random matrix theory (RMT) defined bulk of eigenvalues and that the information extracted at the lower edge is statistically more significant than that extracted from the larger eigenvalues, [9]. The method was applied to multichannel EEG data, where the dynamics of the smallest eigenvalues were shown to be more sensitive to the detection of subtle changes in the brain dynamics than those of the largest eigenvalues.

The use of wavelet techniques in the study of EEG signals is widespread, allowing a time-frequency decomposition of these non-stationary signals. Wavelets, [13–16], were used to determine localisation of transient signals (spikes) during ictal periods, vital in preoperative evaluation of the foci and propagation of ictal events. Furthermore, a wavelet-based similarity method across frequencies was described, using ideas from nonlinear dynamics to predict epileptic seizures, [17].

Various authors have attempted to measure the interdependencies between different regions of the brain. A number of these techniques were compared, with their relative performance shown to be dependent on the form of the underlying signals, [6,7]. In the case of MEG signals, a limited study consisting of three patients was performed, using wavelets to determine cross-correlations over different frequencies and calculate the time lag between different brain regions, [18]. The application of the *coherence function* and cross-correlation between different frequency bands, defined by a continuous filter bank was also used to explore the time-frequency dependence of epileptic seizure data, [19].

In this paper, we seek to expand these techniques through application of time-frequency decomposition to the multivariate analysis of EEG channel interdependency. Data considered are from a number of patients suffering from *focal*, *generalised* or *secondary generalised* epileptic seizures. The frequency dependence of this multivariate technique adds an additional dimension to previous studies, with distinct behaviour of the eigenvalue spectrum and associated correlation between channels demonstrated across different frequencies. The paper is organised as follows. Methods are reviewed in Section 2. In Section 3 we describe the data studied, while in Section 4 we summarise the results obtained and discuss their importance.

2. Methods

2.1. *Correlation Dynamics*

Equal-time cross-correlation matrices between EEG time-series are calculated using a sliding time window where the number of channels, N, is smaller than the window size T. Given EEG time-series $S_i(t)$, $i = 1, \ldots, N$, we normalise these within each window as follows:

$$s_i(t) = \frac{S_i(t) - \widehat{S}_i}{\sigma_i} \tag{1}$$

with σ_i the standard deviation and $\widehat{S}_i$ the time average of S_i over a time window of size T, for channel $i = 1, \ldots, N$.

The equal-time cross-correlation matrix is expressed in terms of $s_i(t)$,

$$C_{ij} \equiv \langle s_i(t)\, s_j(t) \rangle . \tag{2}$$

The elements of C_{ij} are limited to the domain $-1 \leq C_{ij} \leq 1$, where $C_{ij} = 1$ defines perfect positive correlation, $C_{ij} = -1$ corresponds to perfect negative correlation and $C_{ij} = 0$ to no correlation, [1,2]. The correlation matrix can be expressed in matrix notation as

$$\mathbf{C} = \frac{1}{T}\mathbf{S}\mathbf{S}^{\tau} \tag{3}$$

where $\mathbf{S}$ is an $N \times T$ matrix with elements s_{it}.

The eigenvalues λ_i and eigenvectors $\hat{\mathbf{v}}_i$ of the correlation matrix $\mathbf{C}$ are found from the following,

$$\mathbf{C}\hat{\mathbf{v}}_i = \lambda_i \hat{\mathbf{v}}_i. \tag{4}$$

The eigenvalues are then ordered by size, such that $\lambda_1 \leq \lambda_2 \leq \ldots \leq \lambda_N$. The trace of a matrix, ie. the

sum of the diagonal elements, must always remain constant under linear transformation. Thus, the sum of the eigenvalues must always equal the trace of the original correlation matrix, [26]. Hence, if some eigenvalues increase then others must decrease, to compensate, and vice versa.

There are two limiting cases for the distribution of the eigenvalues [8,10]. When all of the time-series are perfectly correlated, $C_i \approx 1$, the largest eigenvalue is maximised with a value equal to N, while all other eigenvalues take value zero. When each of the time-series consists of random numbers with average correlation $C_i \approx 0$, the corresponding eigenvalues are distributed around 1, (where any deviation is due to spurious random correlations).

For cases between these two extremes, we can use the eigenvalue spectrum, calculated using a moving window, to detect changes in the correlation structure. If all channels have an average cross-correlation ρ_0, then the largest eigenvalue is of order $(N-1)\rho_0 + 1$ where N is the number of channels. As this average or *global* correlation between channels increases, the largest eigenvalue increases (to a maximum N), with a corresponding decrease in the small eigenvalues (*eigenvalue repulsion*). Other cases, where correlation structure was more intricate have been described, [8], but in this paper we concentrate on the *global correlation* between channels.

As indicated, the small eigenvalues decrease when the global correlation between channels increases, resulting in a large disparity between the relative size of the small and large eigenvalues. To allow the comparison of eigenvalues from both ends of the spectrum, we normalise each eigenvalue in time using

$$\tilde{\lambda}_i(t) = \frac{\left(\lambda_i(t) - \bar{\lambda}\right)}{\sigma^{\lambda}} \tag{5}$$

where $\bar{\lambda}$ and σ^{λ} are the mean and standard deviation of the eigenvalues over a particular reference period, [10]. This normalisation allows us to visually compare eigenvalues at both ends of the spectrum, even if their magnitudes are significantly different. The reference period used to calculate mean and standard deviation of the eigenvalue spectrum can be chosen to be a low volatility sub-period, (which helps to enhance the visibility of high volatility periods), or the full-time period studied. By normalising the eigenvalues over time, it becomes possible to identify epileptiform events, even using the small eigenvalues.

2.2. *Wavelet Multiscale Analysis*

Wavelets provide an efficient means of studying multiresolution properties, as they can be used to decompose a signal into different time horizons or frequency components. The discrete wavelet transform (DWT), in particular, allows the decomposition of a signal into components of different frequency, [20–22]. There are two basic wavelet functions, the father wavelet ϕ and the mother wavelet ψ. The formal definitions of the father and mother wavelets are the functions:

$$\phi_{j,k}(t) = 2^{\frac{j}{2}} \phi\left(2^j t - k\right) \tag{6}$$

$$\psi_{j,k}(t) = 2^{\frac{j}{2}} \psi\left(2^j t - k\right) \tag{7}$$

where $j = 1, \ldots J$ in a J-level decomposition. The father wavelet integrates to 1 and reconstructs the longest time-scale component of the series, whereas the mother wavelet integrates to 0 and is used to describe the deviations from the trend. The wavelet representation of a discrete signal $f(t)$ in $L^2(R)$ is given by:

$$f(t) = \sum_k s_{J,k}\phi_{J,k}(t) + \sum_k d_{J,k}\phi_{J,k}(t) + \ldots + \sum_k d_{1,k}\phi_{1,k}(t) \tag{8}$$

where J is the number of multiresolution levels (or scales) and k ranges from 1 to the number of coefficients in the specified level. The coefficients $s_{J,k}$ and $d_{J,k}$ are the smooth and detail component coefficients respectively and are given by

$$s_{J,k} = \int \phi_{J,k} f(t) dt \tag{9}$$

$$d_{j,k} = \int \psi_{j,k} f(t) dt \ \ (j = 1, \ldots J) \tag{10}$$

Each of the coefficient sets $S_J, d_J, d_{J-1}, \ldots d_1$ is called a *crystal*.

2.2.1. *MODWT*

The maximum overlap discrete wavelet transform (MODWT) is a linear filter that transforms a series into coefficients related to variations over a set of scale, [22,23]. Like the DWT it produces a set of time-dependent wavelet and scaling coefficients with basis vectors associated with a location t and a unitless scale $\tau_j = 2^{j-1}$ for each decomposition level $j = 1, \ldots, J_0$. The MODWT, unlike the DWT, has a

high level of redundancy, however, and is nonorthogonal. It retains downsampled [1] values at each level of the decomposition that would be discarded by the DWT. The MODWT can also handle any sample size N, whereas the DWT restricts the sample size to a multiple of 2^j. Here, we apply the MODWT as it helps reduce the errors associated with the calculation of wavelet correlation at different scales, (due to the availability of greater amounts of data at longer scales).

Decomposing a signal using the MODWT to J levels theoretically involves the application of J pairs of filters. The filtering operation at the j^{th} level consists of applying a rescaled father wavelet to yield a set of *detail coefficients*

$$\tilde{D}_{j,t} = \sum_{l=0}^{L_j-1} \tilde{\psi}_{j,l} f_{t-l} \tag{11}$$

and a rescaled mother wavelet to yield a set of *scaling coefficients*

$$\tilde{S}_{j,t} = \sum_{l=0}^{L_j-1} \tilde{\phi}_{j,l} f_{t-l} \tag{12}$$

for all times $t = \ldots, -1, 0, 1, \ldots$, where f is the function to be decomposed, [22]. The rescaled mother, $\tilde{\psi}_{j,l} = \frac{\psi_{j,l}}{2^j}$, and father, $\tilde{\phi}_{j,t} = \frac{\phi_{j,l}}{2^j}$, wavelets for the j^{th} level are a set of scale-dependent localized differencing and averaging operators and can be regarded as rescaled versions of the originals. The j^{th} level equivalent filter coefficients have a width $L_j = (2^j - 1)(L-1)+1$, where L is the width of the $j = 1$ base filter. In practice the filters for $j > 1$ are not explicitly constructed because the detail and scaling coefficients can be calculated, using an algorithm that involves the $j = 1$ filters operating recurrently on the j^{th} level scaling coefficients, to generate the $j + 1$ level scaling and detail coefficients [22].

The MODWT is an energy conserving decomposition, [22]:

$$\|\mathbf{f}\|^2 = \sum_{j=1}^{J} \left\|\tilde{\mathbf{D}}_j\right\|^2 + \left\|\tilde{\mathbf{S}}_J\right\|^2 \tag{13}$$

This decomposition allows the measurement of the contribution to the energy due to changes at scale 2^{j-1}. A fractional energy, $\tilde{E}_j$, associated with each scale can be calculated using

$$\tilde{E}_j = \frac{E_j}{E_{tot}}, \; with \; E_{tot} = \sum_{j=1}^{J} E_j. \tag{14}$$

for scales $j = 1, \ldots, J$.

2.2.2. *Wavelet Variance*

The wavelet variance $\nu_f^2(\tau_j)$ is defined as the expected value of $\tilde{D}_{j,t}^2$ if we consider only the non-boundary coefficients [2]. An *unbiased* estimator of the wavelet variance is formed by removing all coefficients that are affected by boundary conditions and given by:

$$\nu_f^2(\tau_j) = \frac{1}{M_j} \sum_{t=L_j-1}^{N-1} \tilde{D}_{j,t}^2 \tag{15}$$

where $M_j = N - L_j + 1$ is the number of non-boundary coefficients at the j^{th} level, [22]. The wavelet variance decomposes the variance of a process on a scale-by-scale basis (at increasingly higher resolutions of the signal) and allows us to explore how a signal behaves over different time horizons.

2.2.3. *Wavelet Covariance and Correlation*

The wavelet covariance between functions $f(t)$ and $g(t)$ is similarly defined to be the covariance of the wavelet coefficients at a given scale. The *unbiased* estimator of the wavelet covariance at the j^{th} scale is given by

$$\nu_{fg}(\tau_j) = \frac{1}{M_j} \sum_{t=L_j-1}^{N-1} \tilde{D}_{j,t}^{f(t)} \tilde{D}_{j,t}^{g(t)} \tag{16}$$

where all the wavelet coefficients affected by the boundary are removed, [22], and $M_j = N - L_j + 1$.

The MODWT estimate of the wavelet cross-correlation between functions $f(t)$ and $g(t)$ may be calculated using the wavelet covariance and the square root of the wavelet variance of the functions at each scale j. The MODWT estimator, [23], of the wavelet correlation is given by:

$$\rho_{fg}(\tau_j) = \frac{\nu_{fg}(\tau_j)}{\nu_f(\tau_j)\nu_g(\tau_j)} \tag{17}$$

[1] Downsampling or decimation of the wavelet coefficients retains half of the number of coefficients that were retained at the previous scale. Downsampling is applied in the Discrete Wavelet Transform

[2] The MODWT treats the time-series as if it were periodic using "circular boundary conditions". There are L_j wavelet and scaling coefficients that are influenced by the extension, which are referred to as the boundary coefficients.

where $\nu_{fg}(\tau_j)$ is the covariance between $f(t)$ and $g(t)$ at scale j, $\nu_f(\tau_j)$ is the variance of $f(t)$ at scale j and $\nu_g(\tau_j)$ is the variance of $g(t)$ at scale j.

2.3. *Defining Seizure Onsets and Endings*

Following [10], we attempted to isolate seizure beginning and end in a reproducible way. First, the absolute slope, $S_i(t) = \left|\frac{\Delta EEG_i(t)}{\Delta t}\right|$, was computed over each channel i. The slope was normalised, $\tilde{S}_i(t) = \frac{S_i(t)}{\sigma_i}$, with σ_i the standard deviation of the signal over a reference period containing no seizure activity. $\tilde{S}_i(t)$ was then smoothed using a moving average over a time window of 5 seconds. *Epiletiform activity* was defined by finding a slope greater then 2.5 standard deviations from the mean, corresponding to periods of extreme neuronal activity, [10]. By calculating the number of EEG channels displaying epileptiform activity, the time of seizure onset was defined. For the following analysis the number of channels needed to signify seizure activity was set to 5, allowing us to isolate periods containing epileptic events.

3. Data

In this study, EEG signals from eight patients of different ages $(28-78)$, determined by a neurologist to be suffering from focal, generalised or secondary generalised seizures were examined. The data was obtained from the Australian EEG database, [24], and all signals were recorded using standard international system $10-20$ electrode placements. The sampling rate for the data was 167Hz, with 23 monopolar channels recorded, (all electrodes have a common reference). The database contains patient details including a history, technician's comments, medication and a full EEG report by a neurologist. The clinical interpretation from the neurologist was used to comparatively classify the seizures. In this analysis only bipolar derivations, (18 bipolar derivations or channels are examined below), between nearest-neighbour channels were used, [25], as the use of monopolar signals might result in the introduction of unwanted correlations into the system.

4. Results

For the present study, we selected the least asymmetric (LA) wavelet, (known as the Symmlet, [20]), which exhibits near symmetry about the filter midpoint. LA filters are defined in even widths and the optimal filter width is dependent on the characteristics of the signal and the length of the data series. The filter width chosen for this study was the LA8, (where 8 refers to the width of the scaling function), since this enables accurate calculation of wavelet correlations to the 5^{th} scale, (given the length of data series available), while still containing enough detail to capture subtle changes in the signal. Although the MODWT can accommodate any level, J_0, the largest level is chosen, in practise, so as to prevent decomposition at scales longer than the total length of the data series, hence the choice of the 5^{th} scale, (Section 2 and [22]).

4.1. *Single Patient Analysis*

We analyse the equal-time cross-correlation dynamics between EEG channels using a sliding window of length $5s$, (chosen so that the signal would be close to stationary during each window). First, the MODWT of each EEG channel was calculated within each window and the correlation matrix between channels at each scale found, (Eqn. 17). The eigenvalues of the correlation matrix in each window were determined, (Eqn. 4), and eigenvalue time-series were normalised in time, (Eqn. 5).

The seizure definition, (Section 2.3), and eigenvalue dynamics for a 30 year old patient suffering from focal epilepsy with possible secondary generalisation are shown, Fig. 1(a). The seizure definition reveals 3 main periods that display epileptiform activity. An initial examination of the eigenvalue dynamics over each of the wavelet scales (corresponding to frequencies from 4Hz to 60Hz), reveals that the *eigenvalue repulsion* found using the equal-time cross-correlation matrix on unfiltered data, [10,11], is also repeated across the different frequencies. Fig. 1(b-f) shows the dynamics of both the largest eigenvalue and that of the average across the 15 smallest eigenvalues. The dynamics of the smallest eigenvalues complement those of the largest eigenvalue, (since the trace of the correlation matrix must remain constant under linear transformation), [8–11], across all scales. As described earlier, the largest eigenvalue increases when the average correlation between channels increases, with a corresponding decrease in the smallest eigenvalues.

In Fig. 1, we see that the largest eigenvalue of the cross-correlation matrix calculated at the highest

frequency ($60Hz$) increases during epileptiform activity. However, as we move to lower frequencies, the largest eigenvalue tends to decrease during epileptiform activity. In this example, the decrease is particularly evident at levels 3 and 4 (corresponding to $15Hz$ and $7Hz$ respectively). The increase in the largest eigenvalue at the highest frequency corresponds to an increase in the average, or global, system correlation at this frequency, with the opposite occurring at lower frequencies, (Section 2.1).

The wavelet energy, (Eqn. 14), measured in a sliding window of $5s$ for each of the wavelet scales, is shown in Fig. 2 for the same patient as previous, (Fig. 1). The energy at the highest frequencies is negligible, *except during periods corresponding to epileptiform activity*, when it increases greatly, corresponding to more than 60% of the total system energy. During non-epileptiform activity, the energy at low frequencies makes up most of the system energy. However, during epileptiform activity the energy at low frequencies drops to negligible levels compensating for the increase at high frequencies implying that most of the system energy is involved in high frequency events such as spikes.

These preliminary results seem to indicate increased levels of correlation between EEG channels at the highest frequencies during epileptiform activity, with corresponding increases in energy. In contrast, the average system correlation at low frequencies, (measured against the dynamical behaviour of the largest eigenvalue), decreases with corresponding decrease in energy. This analysis indicates that high frequencies are of more importance during epileptiform activity, (since the associated energy is higher), and hence the correlation structure at high frequencies may be of more relevance in the characterisation of seizures.

4.2. *Multiple Patient Analysis*

In order to investigate robustness of the initial results further, we examined the eigenvalue dynamics and associated energy for all eight patients described earlier, Section 3, with the individual results shown in Table A.1. For each patient we measured the average eigenvalue size and the associated energy during active periods, (when the largest eigenvalue, at the highest frequency, is greater than 1.5 standard deviations units (SDU) from the mean. This corresponds to the 6.7% largest readings), as well as during normal periods, (when the largest eigenvalue, at the highest frequency, is between -1.5 and 1.5 SDU from the mean). The average eigenvalue size and energy are measured across scales $1-5$, as before. The results for Patient 1 correspond to those shown in Fig. 1.

Fig. 3 shows the distribution of the largest eigenvalue for all patients across each scale. For the highest frequencies, the average eigenvalue is raised considerably during active, when compared to normal periods. Using a Wilcoxon signed-rank test across all samples at each scale, the probability of zero median difference between eigenvalue pairs is less than 0.05 at these frequencies. The raised largest eigenvalues corresponds to an increase in the global or average correlation at these high frequencies. For the lower frequencies, there is a definite overlap between the eigenvalues but with a lower median and much larger variance during the active period.

The energy at each of the scales is shown, Fig. 4, with an obvious increase in energy at the highest frequency during active periods (Wilcoxon signed-rank test, Probability$<$ 0.05 of distributions with the same median). At the next frequency, $30Hz$, the energy is also raised but the behaviour is not as marked. For lower frequencies, the energy decreases during active periods to compensate for the increase at higher frequencies. In particular, for scales 3, the reduction is significant with P$<$ 0.05, (Wilcoxon signed-rank test). This behaviour indicates that the high frequency behaviour is of greatest importance during active periods, with corresponding correlation increase.

5. Discussion

By analysis of the eigenvalue spectrum of EEG epileptiform signals, filtered using the wavelet transform, we were able to examine changes in the eigenspectrum of the cross-correlation matrix between channels. The largest eigenvalue corresponds to the average correlation between all channels and is orthogonal to the other eigenvalues. Previously, a number of studies examined the univariate time-frequency behaviour using a number of different linear and non-linear techniques, [13–16]. However, this single channel approach ignores the interactions between neurons involved in brain activity, particularly prominent during seizures.

Various bivariate methods to examine dynamic changes in these interactions have been suggested. The linear cross-correlation was measured at differ-

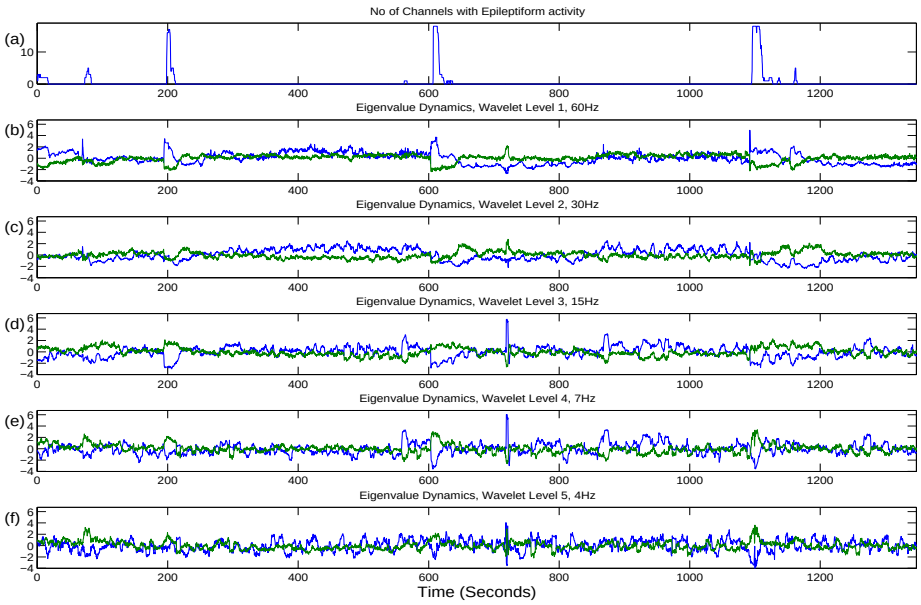

Fig. 1. Patient 1, (a) Seizure definition (b-f) eigenvalue dynamics across first 5 wavelet scales. Blue lines indicate dynamics of largest eigenvalue, while green lines show the average of 15 smallest normalised eigenvalues

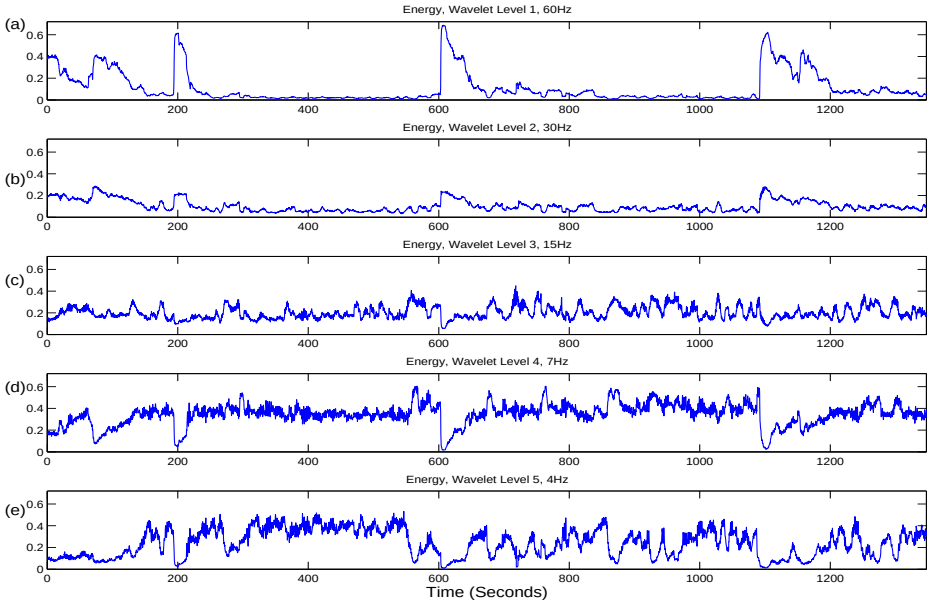

Fig. 2. Patient 1, (a-e) Fractional wavelet energy associated with each of the first 5 wavelet scales, measured using a sliding window of 5s .

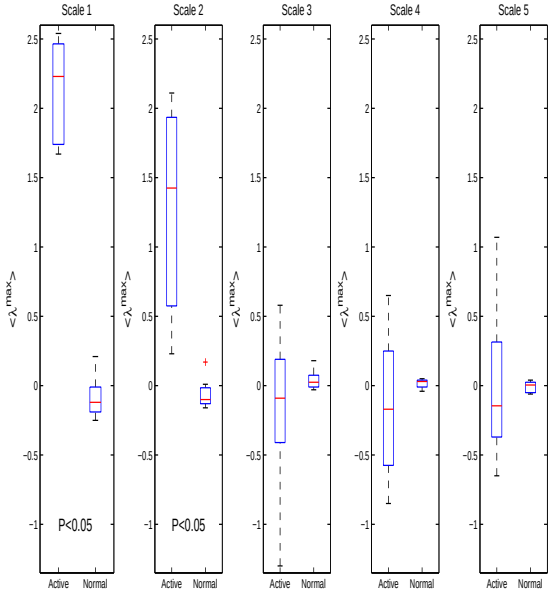

Fig. 3. Largest eigenvalue for all patients across first 5 scales. The red line shows the median value, while the quartiles are shown in blue and outliers as 'whiskers'. The **P** value is the Wilcoxon signed-rank probability (see text).

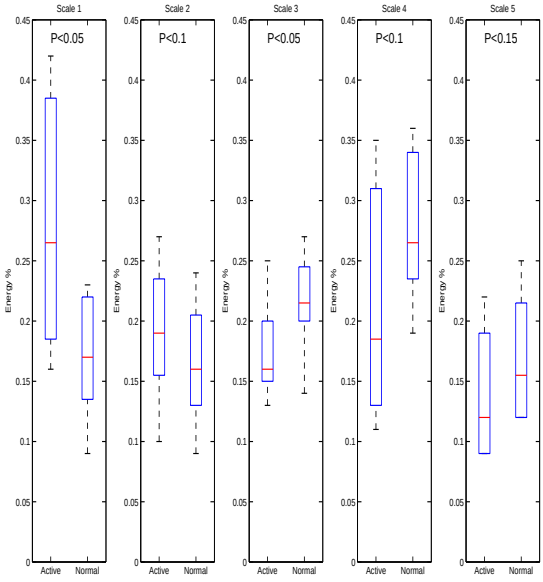

Fig. 4. % Energy for all patients across first 5 scales. The red line shows the median value, while the quartiles are shown in blue and outliers as 'whiskers'. The **P** value is the Wilcoxon signed-rank probability (see text).

ent frequencies, for the channels with the maximum power at high frequencies, [30]. In contrast to the work above, the correlation between these channels was shown to decrease during the seizure. This, however, may be due to the bivariate approach used, which only captured the correlation between particular channels reflecting specific brain regions. This activity may possibly be reflected in the second or third largest eigenvalue of the multivariate technique, where correlations orthogonal to those in the largest eigenvalue are found, (corresponding to correlations between certain subsystems, [8]). The linear cross-correlation for two band-filtered channels were examined for different time lags, with a strong relationship found for a frequency band around 30Hz, [19].

The bivariate methods, described above, concentrated on correlations between a small number of channels, chosen specifically for the study. Using multivariate EEG data, changes in the global correlation structure were shown to be visible at both ends of the eigenvalue spectrum, [8]. For a limited study of a single seizure, a sudden system-wide change from a relatively uncorrelated to highly correlated state was found to take place, reflected in an increase in the largest eigenvalue. Analysis of the changes in the eigenvalue spectrum for a large number of seizures showed a generic change in the correlation structure during focal onset seizures, [10]. The seizure recordings in this data consisted of $58 - 94$ channels and the changes in the eigenvalue spectrum were shown to occur for a number of the largest eigenvalues. Contrary to behaviour found previously, [8], these eigenvalues were shown to decrease during the first half of the seizure, indicating de-correlation, with an increase in correlation found before seizure end. It was suggested that this increase in correlation may be related to seizure termination.

Time-frequency decompositions of EEG signals have been studied for many years, [27]. In this initial work, we extend the previous multivariate techniques, [8,10], by examining changes in the eigenvalues of the correlation matrix between EEG time-series across various frequencies. The results for low frequencies were similar to those found by [10], (see Fig. 1), with a decrease in global correlation at seizure onset, reflected by the decrease in the largest eigenvalue. However, at higher frequencies (Fig. 1(b)), we found an increase in the largest eigenvalue at seizure onset, corresponding to an increase in global correlation. Additional analysis,

across a number of seizures, confirmed that when eigenvalues at the highest frequencies increased, small variation only occured in the correlation at lower frequencies. The limited number of channels available for study, meant that the effects of the global or average correlation were only found in the largest eigenvalue, in contrast to the work by [10].

Previous studies have used wavelet energy in the prediction of seizures, [28]. In our analysis, we examine the fractional energy of each of the frequencies, in order to determine the significance of each over time. This complements the multivariate analysis described, by emphasising the importance of the highest frequencies during active periods. Additionally, it develops the previous work, [8,10], by including frequency insight on the correlation structure over time. By focusing on particular frequencies, a simple multivariate technique such as that described may be applicable to seizure prevention. Additionally, as very high frequency oscillations have been found during seizures, [29], a further study of correlation dynamics at this scale is indicated.

6. Conclusions

Through the use of wavelet multiscaling, we expand the previous multivariate analysis, [8–11], to explore the frequency dependence of the correlation dynamics between EEG channels for patients suffering with different forms of epilepsy. The eigenvalue spectrum of EEG epileptiform signals were filtered using the wavelet transform. Initial analysis, (Section 4.1), consisted of EEG time-series from a patient with focal epilepsy, with results revealing an increase in the largest eigenvalue during epileptiform activity, (corresponding to an increase in correlation between channels), at the highest frequency. In contrast, correlation at lower frequencies decreased during epileptiform activity. Wavelet energy decomposition revealed an increase in energy at higher frequencies during epileptiform activity, with a corresponding decrease at lower frequencies. This implies that *high frequency activity is more significant during epileptiform activity* and hence correlation dynamics at these frequencies assume greater relative importance. The correlation activity at lower frequencies was larger when abnormal activity was low, with higher levels of associated wavelet energy. This suggests that low-frequencies assume greater importance during normal activity.

This approach was then applied to a variety of EEG signals, (Section 4.2), for different types of epileptic activity. *Correlation dynamics were found to be dependent upon the frequency examined, with the correlation structure acting as a barometer of EEG activity.* Clearly, the data available is limited, but the evidence of clear crossover in eigenvalue energy does suggest that monitoring correlation structure in EEG signals at different frequencies can provide a more subtle gauge of incipient imbalance at pre-seizure stage, than is found using unfiltered signals alone.

A more detailed analysis of eigenvalue dynamics at different frequencies during seizures is certainly needed. The work by [10] finds a decrease in overall correlation after seizure start, followed by an increase in correlation as the seizure ends. Our initial results suggest similar behaviour at lower frequencies, while the opposite occurs at higher frequencies. This suggests that the examination of correlation dynamics across various frequencies prior to seizure beginning may reveal pre-seizure characteristics, which can be used to calibrate seizure prevention strategies. An in-depth study on different seizure types may reveal further distinct correlation structures specific to the seizure type. Moreover, analysis of inter-frequency correlations may shed light on the lead-lag relationship across different frequencies, while subsidiary eigenvalue investigation is also worthwhile.

Acknowledgements

The data used in this work was taken from the Australian EEG Database of the University of Newcastle, Australia, [24]. The authors are grateful for the kind assistance of Adam Walker and others associated with the Database.

References

[1] Laloux, L., Cizeau, P., Potters, M., Bouchaud, J., *Random matrix theory and financial correlations*, Int. J. Theoret. & Appl. Finance 3 (3) (2000) 391–397.

[2] Plerou, V., Gopikrishnan, P., Rosenow, B., Amaral, L., Stanley, H.E., *A random matrix approach to cross-correlations in financial data*, Phys. Rev. E 65 (2000) 066126.

[3] Conlon, T., Ruskin, H.J., Crane, M., *Random matrix theory and fund of funds portfolio optimisation*, Physica A 382 (2) (2007) 565–576.

[4] Conlon, T., Ruskin, H.J., Crane, M., *Cross-correlation dynamics in financial time series*, Physica A 388 (5) (2009) 705–714.

[5] Seba, P., *Random matrix analysis of human EEG data*, Phys. Rev. Lett. 91(19) (2003) 198104.

[6] Quian Quiroga, R., Kraskov, A., Kreuz, T., Grassberger, P., *Performance of different synchronization measures in real data: a case study on electroencephalographic signals.*, Phys. Rev. E 65 (2002) 041903

[7] Ansari-Asl, K., Senhadji, L., Bellanger, J-J., Wendling, F., *Quantitative evaluation of linear and nonlinear methods characterizing interdependencies between brain signals*, Phys. Rev. E 74 (2006) 031916

[8] Müller, M., Baier, G., Galka, A., Stephani, U., Muhle, H., *Detection and characterization of changes of the correlation matrix in multivariate time series*, Phys. Rev. E 71 (2005) 046116

[9] Müller, M., Jiménez Y.L., Rummel, C., Baier, G., Galka, A., Stephani, U., Muhle, H., *Localized short-range correlations in the spectrum of the equal-time correlation matrix*, Phys. Rev. E 74 (2006) 041119

[10] Schindler, K., Leung, H., Elger, C.E., Lehnertz, K., *Assessing seizure dynamics by analysing the correlation structure of multichannel intracranial EEG*, Brain 130 (2007) 65–77.

[11] Schindler, K., Elger, C.E., Lehnertz, K., *Increasing synchronization may promote seizure termination: Evidence from status epilepticus*, Clin. Neurophysiol. 118 (9) (2007) 1955–1968

[12] Kwapien, J., Drozdz, S., Ionannides A.A., *Temporal correlations versus noise in the correlation matrix formalism: an example of the brain auditory response*, Phys. Rev. E 62 (2000) 5557

[13] Clark, I., Biscay, R., Echeverria, M., Virues, T., *Multiresolution decomposition of non-stationary eeg signals: a preliminary study*, Comput. Biol. Med. 25 (4) 1995, 373-382.

[14] Senhadji, S., Wendling, F., *Epileptic transient detection: wavelets and time-frequency approaches*, Clin. Neurophyiol. 32 (3) (2002) 175-192.

[15] Adeli, H., Zhou, Z., Dadmehr, N., *Analysis of EEG records in an epileptic patient using wavelet transform*, J. Neurosci. Meth. 123 (2003) 69-87.

[16] Indirdevi, K.P., Elias, E., Sathidevi, P.S., Dinesh Nayak, S., Radhakrishnan, K., *A multi-level wavelet approach for automatic detection of epileptic spikes in the electroencephalgram*, Comput. Bio. Med., 38 (2008) 805-816.

[17] Ouyang, G., Li, X., Li, Y., Guan., X., *Application of wavelet-based similarity analysis to epileptic seizures prediction*, Comput. Bio. Med. 37 (2007) 430-437.

[18] Mizuno-Matsumoto, Y., Ukai, S., Ishii, R., Date, S., Kaishima, T, Shinosaki, K., Shimojo, S., Takeda, M., Tamura, S., Inouye, T., *Wavelet crosscorrelation analysis: non-stationary analysis of neurophyiological signals*, Brain Topogr. 17 (4) (2005).

[19] Ansari-Asl, K., Bellanger, J-J., Bartolomei, F., Wendling, F., Senhadji, L., *Time-frequency characterization of interdependencies in nonstationary signals: application to epileptic eeg*, IEEE T. Bio.-Med. Eng. 52 (7) (2005).

[20] Bruce, A., Gao, H., *Applied Wavelet Analysis with S-Plus* (Springer-Verlag, 1996).

[21] Burrus, C.S., Gopinath, R.A., Gao, H., *Introduction to wavelets and wavelet transforms* (Prentice Hall 1997).

[22] Percival, D.B., Walden, A.T., *Wavelet methods for time series analysis* (Cambridge University press, 2000).

[23] Gencay, R., Selcuk, B., Whitcher, B., *An Introduction to wavelets and other filtering methods in finance and economics* (Academic Press, 2001).

[24] Hunger, M., Smith, R.L.L., Hyslop, W., Rosso, O.A., Gerlach, R., Rostas, J.A.P., Williams,D.B., Henskens, F., *The Australian EEG Database*, Clin. EEG Neurosci. 35 (2) (2005).

[25] Fisch, B.J., Spehlmann, R., *Fisch and Spehlmann's EEG primer: Basic principles of digital and analog EEG*, (Elsevier Health Sciences, 1999).

[26] Jolliffe, I.T., *Principal component analysis, 2nd edition*, (Springer series in statistics, 2002).

[27] Nakata, M., Mukawa, K., *Fourier analysis of broad spectrum EEG from a fluctuation point of view*, Integr. Psychiat. Beh. Sci. 24 (3) (1989) 90-97.

[28] Gigola, S., Ortiz, F., D'attellis, C.E., Silva, W., Kochen, S., *Prediction of epileptic seizures using accumulated energy in a multiresolution framework*, J. Neurosci. Meht. 138 (2004) 107-111.

[29] Bragin, A., Engel Jr., J., Wilson, C.L., Fried, I., Mathern, G.W., *Hippocampal and entorhinal cortex high-frequency oscillations (*$100 - 500 Hz$*) in human epileptic brain and in kainic acid-treated rats with chronic seizures*, Epilepsia 40 (2) (1999) 127-137.

[30] Wendling, F., Bartolomei, F., Bellanger, J.J., Bourien, J., Chauvel., P., *Epileptic fast intracerebral EEG activity: evidence for spatial decorrelation at seizure*, Brain 126 (2003) 1449-1459.

Appendix A

Patient No.	*Scale:*	*1*	*2*	*3*	*4*	*5*
1	Scale 1 Active	2.20	0.23	-1.30	-0.71	-0.33
	Energy	0.38	0.18	0.15	0.17	0.12
	Scale 1 Normal	-0.12	0.01	0.09	0.05	0.03
	Energy	0.09	0.09	0.21	0.36	0.25
2	Scale 1 Active	2.54	1.65	-0.56	0.13	0.52
	Energy	0.39	0.26	0.15	0.11	0.09
	Scale 1 Normal	-0.25	-0.16	0.06	-0.02	-0.05
	Energy	0.23	0.18	0.22	0.19	0.12
3	Scale 1 Active	2.50	2.09	0.58	0.37	1.07
	Energy	0.32	0.27	0.16	0.13	0.12
	Scale 1 Normal	-0.10	-0.08	0.00	0.00	-0.05
	Energy	0.23	0.23	0.19	0.23	0.12
4	Scale 1 Active	1.72	1.78	-0.24	-0.44	-0.11
	Energy	0.42	0.20	0.16	0.13	0.09
	Scale 1 Normal	-0.12	-0.12	0.02	0.03	0.01
	Energy	0.21	0.15	0.26	0.24	0.14
5	Scale 1 Active	2.26	1.20	0.18	-0.31	-0.41
	Energy	0.16	0.16	0.24	0.27	0.17
	Scale 1 Normal	-0.24	-0.13	-0.02	0.03	0.04
	Energy	0.17	0.17	0.23	0.26	0.17
6	Scale 1 Active	2.43	2.11	-0.26	0.65	0.11
	Energy	0.21	0.21	0.16	0.20	0.22
	Scale 1 Normal	-0.14	-0.13	0.03	-0.04	0.00
	Energy	0.12	0.18	0.21	0.27	0.22
7	Scale 1 Active	1.67	0.75	0.06	-0.03	-0.18
	Energy	0.16	0.15	0.25	0.35	0.09
	Scale 1 Normal	0.21	0.17	0.13	0.04	-0.06
	Energy	0.15	0.14	0.27	0.32	0.12
8	Scale 1 Active	1.76	0.40	0.20	-0.85	-0.65
	Energy	0.21	0.10	0.13	0.35	0.21
	Scale 1 Normal	0.08	-0.04	-0.03	0.04	0.02
	Energy	0.17	0.12	0.14	0.36	0.21

Table A.1
Seizure Analysis: Row 1 shows average size of λ^{max} when $\lambda^{max} > 1.5$ at Scale 1, and row 2 the associated energy at each scale. Row 3 shows average eigenvalue at each level when $-1.5 < \lambda^{max} < 1.5$ and row 4 the associated Energy.